

Mining transcriptomic data to study the origins and evolution of a plant allopolyploid complex

Allopolyploidy combines two progenitor genomes in the same nucleus. It is a common speciation process, especially in plants. Deciphering the origins of polyploid species is a complex problem due to, among other things, extinct progenitors, multiple origins, gene flow between different polyploid populations, and loss of parental contributions through gene or chromosome loss. Among the perennial species of *Glycine*, the plant genus that includes the cultivated soybean (*G. max*), are eight allopolyploid species, three of which are studied here. Previous crossing studies and molecular systematic results from two nuclear gene sequences led to hypotheses of origin for these species from among extant diploid species. We use several phylogenetic and population genomics approaches to clarify the origins of the genomes of three of these allopolyploid species using single nucleotide polymorphism data and a guided transcriptome assembly. The results support the hypothesis that all three polyploid species are fixed hybrids combining the genomes of the two putative parents hypothesized on the basis of previous work. Based on mapping to the soybean reference genome, there appear to be no large regions for which one homoeologous contribution is missing. Phylogenetic analyses of 27 selected transcripts using a coalescent approach also are consistent with multiple origins for these allopolyploid species, and suggest that origins occurred within the last several hundred thousand years.

2

Aureliano Bombarely¹, Jeremy E. Coate², and Jeff J. Doyle¹

3 1 - Department of Plant Biology, Cornell University, Ithaca, New York 14853 USA; 2 - Department of Biology, Reed
4 College, Portland, Oregon 97202-8199 USA;

5 INTRODUCTION

6 Polyploidy (whole genome duplication, WGD) is a key process in plant evolution. All seed plants are
7 fundamentally polyploid, with a second WGD event shared by all flowering plants (Jiao et al., 2011), and additional
8 events found in many lineages (see http://genomeevolution.org/wiki/index.php/Plant_paleopolyploidy) (Soltis et al.,
9 2009). It has been estimated that 15% of all flowering plant speciation events involve polyploidy (Wood et al., 2009).
10 Systematists generally recognize autopolyploidy and allopolyploidy as distinct types of polyploidy events, based on
11 the level of divergence of the diploid genomes that formed the polyploid. The terms are best thought of as describing
12 elements of a continuum that ranges from the doubling of a single genome (autopolyploidy), to the incorporation of
13 differentiated genomes in a single nucleus by hybridization of different species (allopolyploidy). From a genetic
14 perspective, allopolyploids are characterized by diploid-like meiotic behavior and limited interaction between the
15 two homoeologous genomes. The duplicated chromosomes of an autopolyploid (and, to a lesser extent, a newly
16 formed allopolyploid; Ramsey and Schemske, 2002) initially can associate randomly, leading to polysomic
17 segregation, but it is generally assumed that this is a transient state; diploidization leads to the eventual presence of
18 homoeologous genomes. It is difficult, if not impossible to determine from the genomes of older polyploids
19 (paleopolyploids, mesopolyploids) how differentiated their progenitor genomes were in large part due to the frequent
20 absence of extant diploid progenitors for comparative purposes.

21 The initial “fixed hybrid” condition of an allopolyploid erodes over time as homoeologous loci are lost
22 (Lynch and Conery, 2000; Maere et al., 2005); this process of “fractionation” is thought to occur preferentially from
23 one subgenome, but the precise mechanisms remain unknown (Schnable and Freeling, 2011; Freeling et al., 2012). In
24 addition to the loss of genes, the process of concerted evolution can result in the replacement of a gene from one
25 genome by its homoeologue, notably through gene conversion (e.g., Wang et al., 2007). The earliest stages of
26 polyploid evolution may contribute disproportionately to gene loss and genomic rearrangement through genomic
27 shock (McClintock, 1984). For example, some individuals of the ca. 100 year-old allopolyploid, *Tragopogon*
28 *miscellus*, have lost entire chromosomes of one parent (Chester et al., 2012). Diversity in polyploids can be due to
29 mutational divergence from parental diploids, but also due to multiple origins produced by different polyploidization
30 events between different genotypes of the same diploid species (Symonds et al., 2010). Questions concerning how
31 polyploids originate (e.g., single vs. multiple origins), how they partition their variation (e.g., as a single lineage
32 united by gene flow vs. as separate lineages formed from different genotypes of the same progenitor species), and
33 how much of the initial parental contributions they retain are among the major questions in polyploid evolutionary
34 research (Soltis et al., 2010).

35 High-throughput sequencing produces massive amounts of genome-wide data, and thus has great potential
36 for systematic and evolutionary studies in general (Gilad et al., 2009). The ready availability of genomic and
37 transcriptomic data has opened new opportunities for studying the evolution of polyploids (Bombarely et al., 2012;
38 Grover et al., 2012; Ilut et al., 2012; Dufresne et al., 2014) at the scale of whole genomes. However, it is not trivial to
39 extract relevant information from short read sequencing data, particularly for allopolyploids, where the interest is
40 often in deconvoluting the complex genome into its two homoeologous subgenomes (Grover et al., 2012; Ilut et al.,
41 2012). Moreover, the field of systematics has what has been called a new paradigm for studying species
42 relationships, involving genealogical approaches (Edwards, 2009). Genealogical methods have lately begun to be
43 applied to both autopolyploids (Arnold et al., 2012; Hollister et al., 2012) and allopolyploids (e.g. Slotte et al., 2011;
44 Jones et al., 2013; Slotte et al., 2013). The confluence of these two developments promises to accelerate the study of
45 polyploid evolution.

46 The genus *Glycine* includes the cultivated soybean (*G. max*) and its wild progenitor (*G. soja*), both annual
47 species native to northeastern Asia, as well as approximately 30 perennial species native to Australia classified as
48 subgenus *Glycine* (Ratnaparkhe et al., 2011). Like many plant species, *Glycine* has a complex history of polyploidy:
49 in addition to events shared with all angiosperms (Jiao et al., 2011) and eudicots (Jiao et al., 2012), the soybean

50 genome retains evidence from a WGD around 50 million years ago (MYA) shared with a large subset of legumes
51 (Blanc and Wolfe, 2004; Schlueter et al., 2004; Cannon et al., 2010), and particularly from a more recent polyploidy
52 event that increased the chromosome number of the ancestor of all extant *Glycine* species from $2n = 20$ to $2n = 40$
53 (Shoemaker et al., 2006; Doyle and Egan, 2010; Schmutz et al., 2010; Doyle, 2012). This *Glycine*-specific WGD
54 occurred between the estimated time of homoeologous gene divergence in the soybean genome (10-13 MYA; e.g.,
55 Egan and Doyle, 2010; Schmutz et al., 2010), and around 5 MYA, when the annual and perennial species diverged
56 from an already-polyploid common ancestor (Doyle and Egan, 2010).

57 In addition to these older events, eight perennial *Glycine* species are allopolyploids with $2n = 78$ or 80 ,
58 hypothesized to have arisen by hybridization involving various combinations of eight extant diploid species, several
59 of them multiple times and involving both progenitors as chloroplast genome donors (Doyle et al., 2004). Various
60 lines of evidence culminated in these hypotheses of reticulate relationships, which are shown in Fig. 1 for the six
61 species that are part of the *G. tomentella* sub-complex (Doyle et al., 2004). Chromosome number polymorphism ($2n$
62 = 38, 40, 78, 80) was observed in what was initially considered a single taxon, *Glycine tomentella* (Newell and
63 Hymowitz, 1978). Patterns of sterility and partial chromosome pairing in artificial crosses among *G. tomentella*
64 plants were consistent with the presence of shared homoeologous diploid genomes among polyploids (Grant et al.,
65 1984; Doyle et al., 1986; Singh et al., 1988). Isozyme studies of diploid and allopolyploid *G. tomentella* led to the
66 characterization of numerous “races” designated either “D” for diploid, or “T” for tetraploid (Doyle et al., 1985;
67 Singh et al., 1998). Morphological complexity, presumably due to the reticulate nature of the complex, has slowed
68 nomenclatural recognition of what are clearly species in the biological sense. More recently, molecular phylogenetic
69 studies assumed a dominant role in refining hypotheses of relationships (Hsing et al., 2001; Singh et al., 1998;
70 Brown et al., 2002; Doyle et al., 2002; Rauscher et al., 2004), and corroborated earlier hypotheses concerning the
71 origins of polyploids from among the diploid ($2n = 38, 40$) “genome groups” that were also initially defined by
72 artificial hybridization studies and later by molecular studies (see Ratnaparkhe et al., 2011). However, these DNA-
73 level studies were based on only two molecular markers: the internal transcribed spacers of the 18S-5.8S-26S nuclear
74 ribosomal gene cistron (nrDNA ITS) and the low copy nuclear gene, histone H3D. Relationships of chloroplast
75 genomes are broadly consistent with these results (Hsing et al., 2001), but are complicated by incongruence with
76 nuclear markers, likely due to a combination of incomplete lineage sorting and introgression (Doyle et al., 2004).
77 Thus, a genome-wide perspective on the origin and evolution of the *G. tomentella* complex, including estimates of
78 dates of origin, has been lacking.

79 A better understanding of the origin and evolution of the *Glycine* allopolyploid complex will complement its
80 exploitation in studying the impact of allopolyploidy on a range of morphological and physiological characters
81 (Coate and Doyle, 2010; Coate et al., 2012; Ilut et al., 2012; Coate et al., 2013; Hegarty et al., 2013). Here we apply
82 phylogenetic and coalescent methods to a transcriptomic dataset from three of these allopolyploid species and their
83 diploid progenitors that was originally generated to study the effects of polyploidy on their ability to cope with stress
84 from excess light (Coate et al., 2013).

85 MATERIAL AND METHODS

86 *Taxon Sampling and Transcriptome Sequencing*

87 Three *Glycine* (Fig. 1) allopolyploid “triads” (from the *Glycine* perennial polyploid complex) defined as an
88 allopolyploid species and its two putative diploid progenitors, were sampled: 1) the allopolyploid, *G. tomentella* T1
89 ($2n = 78$) and the diploid species, *G. tomentella* D1 (E-genome of Hymowitz et al., 2010; $2n = 38$) and *G. tomentella*
90 D3 (D-genome; $2n = 40$); 2) *G. dolichocarpa* (= *G. tomentella* T2; $2n = 80$) and its putative progenitors *G.*

91 *tomentella* D3 and *G. syndetika* (= *G. tomentella* D4; A-genome; $2n = 40$); and 3) *G. tomentella* T5 ($2n = 78$) and its
92 hypothesized progenitors, *G. tomentella* D1 and *G. clandestina* (A-genome; $2n = 40$). Each species was represented
93 by 2-5 accessions sampled from the CSIRO Division of Plant Industry Perennial *Glycine* Germplasm Collection
94 (Table 1). Additionally, a synthetic allotetraploid (A58) was used, which mimics the natural T5 alopolyloid, having
95 been produced by doubling an artificial hybrid of *G. tomentella* D1 (accession G1316) and *G. canescens* (accession
96 G1233; A-genome; $2n = 40$); *G. canescens* is an A-genome species closely related to *G. clandestina*. A summary of
97 the datasets used can be found in Supplementary Table 4.

98 Plants were grown in a common growth chamber with a 12 h/12 h light/dark cycle, 22
99 °C/18 °C day/night temperature regime, and a light intensity of either 125 mmol m⁻² s⁻¹ (LL) or 800 mmol m⁻² s⁻¹
100 (EL). Different light intensities were used for the purposes of a separate study examining light stress responses
101 (Coate et al., 2013). Single leaflets were pooled from six individuals per accession, and RNA-Seq libraries
102 were constructed from the pooled tissue. All samples were taken from approximately 1-week-old, fully
103 expanded leaves, and were collected 0.5–2.0 h into the light period. For each light treatment, all tissue was
104 collected in a single morning and immediately frozen in liquid nitrogen. Total RNA was isolated from pooled
105 leaf tissue using the Plant RNeasy Kit with on-column DNase treatment (Qiagen, Valencia, CA, USA).
106 Single-end RNA-Seq libraries were constructed following the Illumina mRNA-seq Sample Preparation Kit
107 protocol (Illumina, San Diego, CA, USA), with the following modifications: (1) two rounds of polyA
108 selection were performed using the Dynabeads mRNA DIRECT Kit (Life Technologies, Carlsbad, CA, USA); (2)
109 RNA was fragmented for 2 min at 70 °C using the RNA fragmentation reagents kit (Life Technologies; and (3)
110 Illumina PE adapters were replaced with custom-made adapters containing 3nt barcodes in order to facilitate
111 multiplexing of samples (see Coate et al., 2013 for adapters and Supplementary Table S1 for the barcode sequences).
112 Sequencing was performed on either the GAIIX or HiSeq 2000 platform (Illumina), generating 88 nt or 100
113 nt reads, respectively. Equimolar amounts of three (GAIIX) or four (HiSeq 2000) barcoded libraries were
114 combined and sequenced per channel.

115

116 ***Read Processing and Single Nucleotide Polymorphism (SNP) Calling***

117 Reads were processed with Fastq-mcf (Aronesty, 2013) to trim low quality extremes (min. quality 30) and
118 remove short reads (min. read length 50 bp). They were aligned to the soybean genome (version 1.0, downloaded
119 from www.phytozome.net/soybean) using Bowtie2 (Langmead and Salzberg, 2012) with the default parameters.
120 Mapping files from the same accession were merged. Reads without preferential mapping (same score for two or
121 more mapping hits) and with a mapping score below 20 were removed. SNP calling was performed using Samtools
122 (Li et al., 2009). SNPs supported with read coverage below 5 were removed. VCF files were combined and
123 formatted to Structure and Hapmap formats using the Perl script MultiVcfTool
124 (<https://github.com/aubombarely/GenoToolBox/blob/master/SeqTools/MultiVcfTool>).

125 ***Homoeologue read identification and transcript-guided assembly***

126 For homoeologous SNP identification, a consensus diploid transcriptome was rebuilt for each of the species
127 groups (A, with *G. clandestina* and *G. canescens* accessions; D1, with *G. tomentella* D1 accessions; D3, with *G.*
128 *tomentella* D3 accessions; and D4, with *G. syndetika* accessions) using Samtools (Li et al., 2009) and Gffread from
129 the Cufflinks software package (Trapnell et al., 2010). A progenitor reference set was created for each of the
130 polyploid species joining the diploid transcriptome sets (T1=D1+D3, T2=D3+D4 and T5=A+D1). Reads from the
131 polyploid species were mapped with these references using Bowtie2. Sam mapping files were processed to identify
132 reads according the preferential mapping with each of the progenitors using the Perl script, SeparateHomeolog2Sam
133 (<https://github.com/aubombarely/GenoToolBox/blob/master/SeqTools/SeparateHomeolog2Sam>). Reads with

134 mapping score AS and XS = 0 (No SNPs) were kept and used to rebuild the polyploid transcriptomes using Samtools
135 (Li et al., 2009) and Gffread (from the Cufflinks package, Trapnell et al., 2012). Once the reads were separated
136 according its preferential mapping, they were mapped back to the soybean genome. SNPs were called as described
137 above.

138 *Population structure analysis*

139 The programs Structure (Pritchard et al., 2000) and fineStructure (Lawson et al., 2012) were used to analyze
140 population structure of the two SNP datasets, with and without polyploid SNPs separated by homoeologue, described
141 above. For Structure, each of the datasets was divided into three subsets of 20,000 SNPs selected with a random
142 function incorporated in the MultiVcfTool. 5 replicates were run for each of the subsets with a burn-in of 10,000 and
143 a number of MCMC repetitions of 10,000, from K=1 to K=15 using the default parameters ($\lambda=1$, assuming uniform
144 distribution of allele frequencies, Pritchard et al., 2000). Admixture was selected. The optimal number of clusters
145 was identified based on the rate of change in the log probability of data between successive K values (Evanno et al.,
146 2005). Results at K=6 were verified with a re-analysis using a burn-in of 100,000 generations. Results were
147 visualized using R (barplot function).

148 The two SNP datasets were divided into 20 different subsets each mapping to one soybean reference
149 chromosome for FineStructure analysis. Analyses were performed following the instructions from the fineStructure
150 web for the unlinked model (http://www.maths.bris.ac.uk/~madjl/finestructure/data_example.html). Results were
151 presented as a heatmap of distances between each of the accessions. A principal component analysis (PCA) was
152 performed over the same distance matrix using fineStructure software. The PCA figure was created using R.

153 *Reconstruction of phylogenies using concatenated SNPs*

154 SNPs from the dataset in which SNPs from allopolyploids were partitioned into their two homoeologues
155 (“homoeologue data set”) and were concatenated to create a supermatrix with 36 operational taxonomic units
156 (OTUs). The two homoeologous gene copies from each allopolyploid were treated as individual OTUs; for example
157 the D1 and D3 homoeologues of T1 individuals were treated as D1T1 and D3T1, respectively. *G. max*, accession
158 William82 was used as outgroup. The alignment files were produced changing the SNPs Hapmap format to fasta
159 using a Perl script. The resulting matrix was used in two analyses. First, maximum likelihood (ML) was used,
160 implemented in PhyML (Guindon and Gascuel, 2003) with GTR as the substitution model; 100 bootstrap replicates
161 were conducted. Second, in order to visualize reticulations in the dataset, a network method, NeighborNet, was
162 implemented in the SplitsTree package (Huson and Bryant, 2006) with the default parameters. Trees were visualized
163 and drawn using FigTree (Rambaut, 2012).

164 *Gene-based analyses*

165 A subset of transcripts was selected for phylogenetic and network analyses based on the following criteria:
166 No more than 10% of Ns for the guided assembly consensus sequence in any of the accessions after the
167 homoeologue read identification; alignments with at least 1000 bp; and genes with their corresponding *G. max*
168 homologue identified as an existing pair retained from the most recent (ca. 5-10 million years; (Doyle and Egan,
169 2010)) *Glycine* WGD event, as compiled by Du et al. (Du et al., 2012). Sequence alignments were based on the
170 transcriptome-guided assembly. Sequence for each of the genes was collected with a Perl script (FastaSeqExtract,
171 GenoToolBox script package), concatenated and changed to the required sequence alignment format using a BioPerl
172 script (bp_sreformat.pl). The 95 alignments selected were used in an exploratory phylogenetic analysis using the

173 Bayesian MCMC method, BEAST (Drummond et al., 2012) (HKY substitution model, 10,000,000 MCMC).
174 Alignments that produced trees in which *G. max* was not sister to perennial *Glycine* species in the consensus tree
175 were removed. Generally the removed alignments showed tree topologies with two large clades with long branches,
176 indicating the possibility of inclusion of paralogous genes from the older whole genome duplication (ca. 50 MY,
177 common to the Leguminosae; reviewed in Doyle 2012) instead the orthologue.

178 27 genes selected after this filtering were analyzed using three different methods: 1) Phylogenies were
179 reconstructed using ML using PhyML (Guindon and Gascuel, 2003) with 1,000 bootstraps. jModelTest2 was used to
180 choose the best substitution model (Darriba et al., 2012). According to the Bayesian Information Criterion (BIC)
181 HKY was the preferred model (40% of the genes), followed by K80 (26% of the genes; Supplementary Table S2). 2)
182 Networks were constructed using NeighborNet in SplitsTree4 with the default parameters (Huson and Bryant, 2006).
183 3) Bayesian analysis was performed using BEAST v2.0 (Drummond et al., 2012). The two homoeologous gene
184 copies from each allopolyploid were treated as individual OTUs as in the concatenated analysis, and *G. max*,
185 accession William82 was again used as outgroup. Based on the jModelTest2 results, HKY was used as the
186 substitution model. The MCMC chain was set to 100,000,000 MCMC generations, taking samples every 1000
187 generations. Divergence ages were estimated by scaling the tree root (divergence between *G. max* and perennials) to 5
188 Myr (Egan and Doyle, 2010). All trees were drawn using FigTree (Rambaut, 2012).

189 *Species tree reconstruction*

190 Species tree reconstruction under the coalescent was performed using the 27 selected genes in *BEAST
191 (Drummond et al., 2012). The 24 accessions, including two homoeologues for each allopolyploid accession, were
192 grouped in 11 operational taxonomic units (OTUs) for this analysis: *G. canescens*, *G. clandestina*, *G. tomentella* D1,
193 *G. tomentella* D3, *G. syndetika* (D4), *G. tomentella* T1-D1, *G. tomentella* T1-D3, *G. dolichocarpa* T2-D3, *G.*
194 *dolichocarpa* T2-D4, *G. tomentella* T5-A and *G. tomentella* T5-D1. *G. max* was used as outgroup. Based on
195 jModelTest2 results, HKY was used as substitution model. The MCMC chain was set to 100,000,000 MCMC
196 generations, taking samples every 1000 generations. Divergence dates were estimated as described above. All the
197 trees were drawn using FigTree (Rambaut, 2012).

198 **RESULTS**

199 *Phylogenomics dataset generation*

200 Between 7-60 million reads from leaf transcriptomes of 24 accessions representing 8 *Glycine* perennial
201 species were mapped to the *Glycine max* genome (v1.0) (Schmutz et al., 2010). Reads mapped to 22,500-25,000
202 genes (~40% of soybean gene models; Table 1); this represents between 4.5 and 11.6% of the genome. 200,000-
203 965,000 single nucleotide polymorphisms (SNPs) were identified relative to *G. max*; 6.3-12.6% of SNP positions
204 were polymorphic in diploid species (*G. clandestina*, *G. canescens*, *G. tomentella* D1 (referred as D1 hereafter), *G.*
205 *tomentella* D3 (referred as D3) and *G. syndetika* (referred as D4)), and 18.4-28.8% in polyploid species (*G.*
206 *tomentella* T1 (referred as T1), *G. tomentella* T5 (referred as T5) and *G. dolichocarpa* T2 (referred as T2); Table 2).
207 The interpretation of these positions as standard heterozygosity is complicated by the recent (5-10 MYA: Doyle and
208 Egan, 2010) WGD in the ancestral *Glycine* genome. In a gene for which soybean has lost one of the homoeologous
209 copies from this event, but the perennial species for which it is serving as reference has retained both copies,
210 polymorphic SNPs may be due to reads from two different homoeologous loci in the perennial, rather than two
211 alleles at a single locus. Low levels of conventional heterozygosity are expected in *Glycine* species, because of their
212 strongly selfing reproductive biology, with much reproduction occurring through cleistogamous (closed, selfing)

213 flowers.

214 The much higher percentage of polymorphic positions in polyploid individuals (T1, T2, T5) likely is also
215 due to the mapping of reads from two homoeologous copies to a single target, in this case due to recent polyploidy:
216 for example, mapping reads from tetraploid ($2n = 80$) T2 to a single locus in the diploid ($2n = 40$) *G. max* reference
217 genome will result in reads from both its D3 and D4 homoeologous subgenomes mapping to the same target,
218 increasing the chance of observing a polymorphism at a given site. Separating reads from T1, T2, and T5 polyploid
219 individuals was possible where the read has at least one SNP that could be related to one homoeologous genome
220 contributor (e.g., D3 and D4 differed by a SNP and this difference was retained in the D3 and D4 homoeologous
221 genomes of T2; diploid-distinguishing polymorphism (DDP; see Ilut et al., 2012). Between 11.4 and 20.8% of reads
222 were assigned to one of the progenitors (Table 3).

223 Between 124,984 and 399,884 SNPs were produced for each accession. The filtering of the missing data
224 produced 237,243 and 75,958 polymorphic positions for all the accessions before and after the homoeologous read
225 assignment, respectively. SNPs per chromosome ranged from 7,455 (chromosome 14) to 16,494 (chromosome 8) and
226 from 2,288 (chromosome 14) to 5,300 (chromosome 8) before and after the homoeologous read assignment,
227 respectively.

228 Transcriptome-guided assemblies produced between ~1,800 and ~6,600 full-length sequences (as mapped to
229 the *G. max* gene models) for each diploid accession. For polyploid subtranscriptomes this number was much lower
230 because only reads that mapped preferentially to one of the diploid consensus species and reads that mapped equally
231 but with no polymorphism (perfect match) were used during the transcriptome-guided assembly. Any read that
232 mapped equally to two or more positions with one or more polymorphisms was discarded because it was impossible
233 to assign it to any of the diploid progenitors, reducing the mapping coverage of the reference gene models. Between
234 ~350 and ~1,350 full length sequences were assembled for the T1, T2, and T5 polyploid homoeologous
235 subtranscriptomes of which between 4 to 19% were duplicated genes from the 5-10 MYA WGD event in the
236 common ancestor of *Glycine* species (Schmutz et al., 2010). For phylogenetic analysis, full length sequences are not
237 needed so a phylogenetic analysis dataset was created with 27 genes (see Material and Methods for the criteria used
238 to generate this dataset; Table 5).

239 ***Genome-wide distribution of homoeologous SNPs.***

240 For each allopolyploid accession, the ca. 120,000-400,000 SNPs (Table 3) that could be identified to
241 homoeologous subgenome were mapped to the soybean reference genome (Schmutz et al., 2010). This produced a
242 map that is analogous to chromosome painting (genomic in situ hybridization, GISH) experiments using the reads
243 from which the SNPs were derived, which we term “electronic chromosome painting” (e-chromosome painting).
244 Similar patterns were seen for all accessions, with high densities of SNPs at the ends of each soybean chromosome
245 and far lower densities in pericentromeric regions (Fig. 2). This pattern is expected using reads from transcriptome
246 data, because of the sparse distribution of genes in pericentromeric regions of the soybean genome (Schmutz et al.,
247 2010). Notably, in all allopolyploid accessions, SNPs from both homoeologues were distributed across the entire
248 genome, and no regions were identified in which SNPs from only one homoeologue were mapped (Fig 2;
249 Supplementary Figs. 1-10).

250 ***Population structure analyses.***

251 Structure (Pritchard et al., 2000) was first run using all available SNPs, without separating SNPs from
252 polyploids into homoeologous groups. Structure was run from $K = 1-15$; $K = 6$ was identified as one of the optimal
253 preferred values of K using the delta K method of Evanno et al. (2005; Supplementary Fig. 11). Five of these six

254 groups corresponded to diploid taxa: D1, D3, D4, *G. canescens*, and *G. clandestina* (Fig. 3a). The sixth group was
255 represented only as a minor component in D4 accession 2073. Diploid accessions showed little or no evidence of
256 admixture, with the exception of D4 accession 2073 (Fig. 3). In contrast, all polyploid accessions were admixed,
257 each with approximately 50% contributions from two different diploid groups. The genomic makeup of each
258 accession was as expected from previous hypotheses (e.g., Doyle et al., 2002; Fig. 1): T1 accessions showed
259 admixture from D1 and D3, T2 accessions from D3 and D4, and natural T5 accessions from D1 and *G. clandestina*.
260 The synthetic T5 accession (A58) was also admixed, with contributions from D1 and *G. canescens*, as expected (Joly
261 et al., 2004).

262 A second Structure analysis was conducted with each polyploid accession treated as two separate OTUs,
263 using the homoeologue dataset (Table 2). As with the previous analysis, the analysis was run for $K = 1-15$. The
264 Evanno method (Evanno et al., 2005) identified $K = 6$ and 9 as the preferred values (Supplementary Fig. 11). In the
265 case of $K = 9$ the group representation shows the same structure than the $K = 6$ (Supplementary Fig. 12). Results for
266 diploids were similar to those obtained in the previous analysis (Fig. 3b). Subgenomes from natural allopolyploids
267 and the synthetic T5 allopolyploid (A58) were shown to belong exclusively to diploid groups, with little or no
268 evidence of admixture, indicating that the SNP filtering into homoeologous contributions was successful.

269 Complementary to the second Structure analysis, the data were analyzed using ChromoPainter and
270 FineStructure (Lawson et al., 2012). ChromoPainter produces a co-ancestry matrix (as a measure of the ancestry
271 sharing between individuals) based on the haplotype information provided by shared chunks (regions) of biallelic
272 markers between individuals (Lawson et al., 2012). The two SNP datasets were filtered by selecting only the biallelic
273 markers, producing a subset with 220,952 and 71,610 SNPs (before and after homoeologous read assignment,
274 respectively) distributed along all 20 soybean chromosomes. Regions identified by ChromoPainter for each
275 accession ranged from 516 (D4 2321) to 567 (*G. clandestina* 1253) and from 202 (D4 1300 and 2321) to 221 (D4
276 2073) (before and after homoeologous read assignment respectively). Principal component analysis (PCA) and
277 population relationship analysis using a Bayesian approach were performed over the co-ancestry matrix using
278 FineStructure (Lawson et al., 2012). PCA before homoeologous read assignment (Fig. 4a) shows seven well-
279 differentiated groups, one per species with the exception that *G. canescens* and *G. clandestina* clustered together.
280 Diploid species formed the vertices of a trapezoid. A-genome species (*G. canescens*, *G. clandestina* and D4) formed
281 a more dispersed group than either D1 or D3. Each polyploid species fell between its putative diploid progenitors,
282 consistent with each being an admixture (fixed hybrid). After the homoeologous read assignment (Fig. 4b), each of
283 the polyploid subgenomes clustered with its diploid progenitors, producing three clear clusters: D1, D3, and A-
284 genome (comprising *G. canescens*, *G. clandestina* and D4, as expected). Heatmaps were used to visualize the
285 population relationships produced by FineStructure, complementing the information shown by the PCA figures. The
286 heatmap before homoeologous read assignment (Fig. 4c), showed four intense regions (red, magenta and blue colors)
287 corresponding to the four species groups of the PCA (Fig. 4a). Each polyploid showed the expected similarity to its
288 progenitors; similarly, as expected the two *G. clandestina* accessions were more similar to one another than either
289 was to *G. canescens*. Also, T5 A58, the artificial polyploid produced from a cross between *G. canescens* 1232 and
290 D1 1316, showed the expected relationships with these accessions. Other T5 polyploids also showed a stronger
291 signal from D1 1316 than from other D1 accessions. T2 accessions did not show any stronger signal with any
292 particular D3 accession than with others, but they did with the D4 accessions 1300 and 2321, relative to 2073. T1
293 accessions 1288 and 1763 also showed a stronger signal with particular D1 and D3 accessions, whereas T1 accession
294 1361 showed a weaker signal with the D1 and D3 accessions included here. After the homoeologous read assignment
295 (Fig. 4d), some of these signals were intensified, such as the relationship between T5-D1 subgenomes and particular
296 D1 accessions, but other relationships that were suggested when all SNPs were considered were not observed (for
297 example there is not a stronger signal of D1 1316 with the T5 accessions). These differences may be due to the
298 methodology used for the homoeologous read assignment.

300 Phylogenetic and network analyses were conducted using the homoeologue dataset, with SNPs
301 concatenated to create a single supermatrix. The maximum likelihood (ML) tree, rooted with *G. max*, identified four
302 subclades comprising two major clades: 1) the A-genome, with subclades of D4 vs. *G. clandestina* and *G. canescens*;
303 and 2) the D-genome (D3) and E-genome (D1) (Fig. 5a). Each of the subclades showed a different pattern with
304 respect to diploid and tetraploid subgenome relationships. In the *canescens/clandestina* clade, the A-subgenome of
305 the synthetic allopolyploid (A58) was sister to the accession from which it was created (*G. canescens* 1232), as
306 expected, though with deeper coalescence than expected from an artificial hybrid; the two natural T5 allopolyploids
307 were sister to *G. clandestina* 1126, as expected from other data (e.g., Doyle et al. 2002). In the D4 clade, diploid
308 accession 2073 was sister to all remaining accessions, a unique placement consistent with its apparently admixed
309 nature (Fig. 3a). The polyploid subgenomes formed a paraphyletic group, with the two diploid accessions sister to
310 the D4 subgenome of one T2 accession (1134). A similar pattern was seen in the D3 subclade, where T2 accessions
311 formed a paraphyletic group, and all four diploid accessions formed a clade sister to T2 accession 1134. Also
312 embedded within the T2 accessions was a clade consisting solely of T1 accessions. T1 accessions also formed a
313 monophyletic group within the D1 clade, where natural T5 accessions and D1 accessions also formed monophyletic
314 groups. Surprisingly, there was not a sister relationship between the D1-subgenome of synthetic allopolyploid A58
315 and the D1 accession from which it was formed (1316). Similar topologies were produced by neighbor-joining
316 analysis (data not shown).

317 NeighborNet was used to analyze the full homoeologue dataset to identify minority patterns of relationships
318 in the data. When rooted with *G. max*, the topology (Fig. 5b) was very similar to the ML tree (Fig. 5a), even having
319 such features as the sister relationship of D4 2073 to other D4 accessions, and the monophyly of T1 homoeologues in
320 both the D1 and D3 clades. There was clear evidence of character support for alternative relationships, but those
321 relationships were minor in comparison with the major phylogenetic signal.

322 *Gene-based phylogenetic and network analyses*

323 Gene trees were constructed for the 27 genes (described in the Material and Methods) using several
324 different phylogenetic and network methods. Similar topologies for trees from individual genes were obtained with
325 BEAST and PhyML. All 27 trees showed the split between the A-genome clade and the D1/D3 clade seen in the ML
326 tree reconstructed from concatenated SNPs (Fig. 5a). However, many individual gene trees showed unexpected
327 groupings of one or more accessions, particularly within the A-genome clade, where several trees grouped accessions
328 from *G. canescens* with *G. syndetika*-D4 instead of with *G. clandestina* (for example ML and BEAST trees for the
329 gene Glyma04g39670, Supplementary Figs. 17 and 45). Relationships within the major subclades varied among the
330 27 gene trees. For example, nine of the 27 trees showed separate clades for *G. canescens* (plus the A58 sequence)
331 and *G. clandestina* (e.g., Fig. 6, a and c), but in only three of them did diploid species form monophyletic groups
332 (Supplementary Figs. 13-67). Overall, there were far more departures from expectations in the A-genome clade than
333 in the D1/D3 clade.

334 There were numerous cases where alleles from diploid accessions formed monophyletic groups (e.g., 12 of
335 27 BEAST topologies had alleles from all four D3 accessions in a clade, often with high posterior probability). At
336 some loci, alleles from one or more polyploids formed monophyletic clades; for example, at Glyma06g18640
337 (Supplementary Fig. 50), all taxa, including both homoeologous subgenomes of each polyploid, formed separate
338 clades, with the exception of *G. clandestina*. However, this was unusual, and paraphyletic groupings of alleles were
339 common, particularly in polyploids. For example, at 26 of 27 loci, T2-D3 alleles were not monophyletic, at least
340 some having closer relationships to D3 or T1-D3 alleles, and in gene Glyma01g35620, T5-D1_1969 was most
341 closely related to D1_1156 whereas T5-D1_1487 was most closely related to D1_1157 and D1_1316 (Supplementary
342 Fig. 41). On the assumption that alleles in tetraploids all originated from diploid progenitor species, such

343 paraphyletic relationships suggest the input of alleles from different genotypes of diploid progenitors, due either to
344 multiple origins or, alternatively, to continued gene flow from diploids after polyploid formation, perhaps involving
345 unreduced gametes.

346 The BEAST trees, calibrated with the 5 MYA divergence of *G. max* and the perennial subgenus (Innes et al.,
347 2008), allowed dates of allele divergence to be estimated. Among comparisons of interest are the minimum
348 divergences between alleles from a tetraploid and alleles from its diploid progenitor (e.g., T2-D3 vs. D3) or alleles
349 from the same progenitor in a second tetraploid (e.g., T2-D3 vs. T1-D3); the latter represent “diploid” alleles as well,
350 under the assumption that there has been no gene flow between the two tetraploids, something that is reasonable for
351 *G. tomentella* tetraploids (e.g., Doyle et al. 1986). Minimum distances between polyploid and diploid alleles
352 (over)estimate the time of entry of that allele into the polyploid, which is typically assumed to be an origin of the
353 polyploid (Doyle and Egan 2010). Minimum dates (Supplemental Table 3) were 0.31 MY for T1 (measured at the D1
354 locus), 0.29 MY for T5 (measured at the D1 locus), and 0.38 MY for T2 (measured at the D3 locus). Error bars on
355 these estimates, however, were substantial.

356 NeighborNet (implemented in SplitsTree 4; Huson and Bryant, 2006) was used to construct networks for
357 each of the 27 genes. Several networks showed patterns consistent with intragenic recombination; the Pairwise
358 Homoplasy Index (PHI) of Bruen et al. (2006), also implemented in SplitsTree, was significant for 11 of the 27 genes
359 (data not shown). The dominant patterns in NeighborNet topologies were similar to the overall pattern shown in
360 phylogenetic analyses of the 27 genes, and thus to results for the full homoeologous SNP dataset. As with other
361 methods, NeighborNet networks suggested multiple inputs of alleles from diploid progenitors into polyploids (e.g.,
362 gene Glyma02g11580, Fig. 6c).

363 *Species tree reconstruction under the coalescent*

364 Species trees were reconstructed using the coalescent approach implemented in *BEAST (Heled and
365 Drummond, 2010), which used information contained in the individual gene trees from the 27 genes described
366 above. The overall *BEAST tree (Fig. 7a) topology was similar to that of trees from concatenated SNPs. By
367 definition, each of the allopolyploid homoeologous genomes was a single OTU despite the possibility of independent
368 origins; each of these was grouped with its putative progenitor species. Within the D1 genome clade, the T1 and T5
369 polyploids were sisters to one another; similarly, T1 and T2 were sisters in the D3 clade. The DensiTree output
370 (Supplementary Fig. 40) indicated considerable uncertainty only within the D3 clade, where both other possible
371 topologies (T2 sister to D3, T1 sister to D3) appeared in a substantial number of trees. As expected, divergence dates
372 of polyploids from their diploid progenitors estimated by *BEAST were higher than minimum estimates from the 27
373 individual loci, all being greater than 300,000 years (Fig. 7a).

374

375 **DISCUSSION**

376 The *Glycine* subgenus *Glycine* polyploid complex appears ideally suited as a model for studying
377 allopolyploid evolution, because it comprises eight independently formed but closely related allopolyploid species
378 triads (an allotetraploid and its two diploid progenitors; Fig. 1) that overlap in their genomic compositions. We are
379 exploiting this model system to study the effect of allopolyploidy on a wide range of phenotypes, including
380 transcriptome size, morphology, anatomy, climate niche, photosynthesis, and photoprotection (Coate and Doyle,
381 2010; Coate et al., 2012; Ilut et al., 2012; Coate et al., 2013; Coate and Doyle, 2013; Hegarty et al., 2013; Coate et
382 al., 2014; Harbert et al., 2014).

383 To enhance the utility of this model group, it is important to move to a genome-wide understanding of their

384 biology. As noted above, origins of the *Glycine* allopolyploids were hypothesized initially from crossing data and
385 more recently from gene phylogenies, but inferences have been made from only two nuclear genes. Both of these
386 markers supported the hypotheses of fixed hybridity of *Glycine* allopolyploid species. However, it is not known to
387 what extent the entire genomes of these plants retain contributions from both parental diploid species in the face of
388 potential loss due to initial genomic shock (McClintock, 1984), or other processes such as “genome downsizing”
389 (Leitch and Bennett, 2004), fractionation (Schnable and Freeling, 2011; Freeling et al., 2012), or concerted evolution
390 (e.g., Wang et al., 2007).

391 ***Glycine* allopolyploids are fixed hybrids throughout their genomes**

392 Analyses using all SNPs identified from the full dataset showed that all three of these allopolyploids are
393 indeed fixed hybrids, combining diploid genomes as depicted in Fig. 1. Structure results indicated an essentially
394 equal contribution from both parental diploids in all three cases (Fig. 3a); PCA analysis also was consistent with this
395 hypothesis, placing each polyploid approximately midway between its putative progenitors, as expected for an F1
396 hybrid (Fig. 4a).

397 In order to determine whether or not the polyploids have contributions from their parents across their entire
398 genomes, reads were partitioned by homoeologous genome and mapped to the soybean reference genome (Schmutz
399 et al., 2010). As portrayed by e-chromosome painting (Fig. 2), it is clear that no individual sampled from any of the
400 three allopolyploid species has any major regions represented by only one homoeologue. Coverage is sparse in
401 pericentromeric and centromeric regions, as expected due to the low density of genes in these regions of the soybean
402 genome (Schmutz et al., 2010). The degree of shared synteny between soybean and these perennial *Glycine* species
403 is as yet unknown, but regardless of the order of chromosomal segments, it is clear that there has not been significant
404 loss of homoeologous genes. We mapped reads to over 22,000 of the approximately 46,000 genes of the soybean
405 genome (Schmutz et al., 2010). These numbers include both homoeologous copies from the 5-10 MYA polyploidy
406 event that shaped the modern “diploid” ($2n = 38,40$) *Glycine* genome. We were able to deconvolute between 4 and
407 19% of these 22,000 genes into their homoeologous contributions in each of the three recent allopolyploids (e.g.,
408 T1D1 and T1D3). Using genomic in situ hybridization (GISH), Chester et al. (2012) showed examples of
409 allopolyploid *T. miscellus* plants that had all four chromosomes or chromosome segments of one diploid parent (4:0),
410 but also examples of plants with 3:1 ratios of homoeologous chromosomes or chromosomal segments. Our e-
411 chromosome painting method cannot distinguish the 3:1 condition from an equal contribution from both parents
412 segments, so it is possible that such plants exist in our sample.

413 Structure analysis using the partitioned homoeologous SNPs corroborated results with the full, unpartitioned
414 dataset, in placing each polyploid homoeologous genome with its putative progenitor (Fig. 3b). The FineStructure
415 PCA supported three major groupings, each of which included diploids and the expected polyploid homoeologous
416 subgenomes derived from them (Fig. 4b). The grouping of D4 accessions and two A-genome species (*G. canescens*
417 and *G. clandestina*), along with polyploid genomes derived from them, into a single cluster is not surprising, because
418 *G. syndetika* (D4) is also a member of the A-genome (Ratnaparkhe et al., 2011). As noted above, genome groups
419 were originally defined on the basis of reproductive compatibility in artificial crosses (Ratnaparkhe et al. 2011), and
420 indeed *G. syndetika* (D4) 2073 shows evidence of admixture with *G. canescens* and *G. clandestina* (Fig. 3). In
421 contrast, D1 and D3, though both classified as “*G. tomentella*”, belong to two different genome groups (E and D,
422 respectively; Ratnaparkhe et al. 2011). This greater genetic similarity of the three A-genome species is not reflected
423 in relative divergence dates; for example, the *BEAST analysis dates the divergence between *G. syndetika* and the
424 two other A-genome species at slightly earlier than the divergence between D1 and D3 (Fig. 7a). Thus, reproductive
425 barriers likely arose earlier in the D1/D3 lineage than within the A-genome.

426 Allopolyploid evolution in *Glycine* fits “Darlington’s Rule” (Darlington, 1937)—that allopolyploids should
427 form between species that are reproductively isolated, often due to chromosomal differences, whereas reproductively

428 compatible diploids instead tend to form homoploid hybrids. No allopolyploids are known to have formed among A-
429 genome species, and only one of the eight known *Glycine* allopolyploids involves hybridization within a genome
430 group (tetraploid *G. tabacina* is the product of the most divergent species cross possible within the B-genome; Doyle
431 et al., 2004). D1 and D3, which as noted belong to different genome groups, have different chromosome numbers
432 ($2n = 38$ vs. 40 , respectively), which may contribute to their inability to form fertile diploid hybrids. D1 has also
433 formed allopolyploids with D5A, another $2n = 40$ "*G. tomentella*"; however, reproductive incompatibility also
434 occurs between $2n = 40$ *G. tomentella* taxa (Doyle et al., 1986), and other allopolyploids in the complex combine
435 genomes of two $2n = 40$ taxa (Fig. 1).

436 ***Gene histories, allele divergence times, and sources of genetic diversity in polyploids.***

437 Gene trees from the 27 loci were selected that met criteria designed to provide orthologues. These genes are
438 highly transcribed with sufficient characters for phylogeny reconstruction, and inferences of polyploid origins mostly
439 conformed to expectations based on previous work using the low copy nuclear locus, histone H3D (Brown et al.,
440 2002; Doyle et al., 2002; González-Orozco et al., 2012), the nrDNA ITS (Singh et al., 2001; Rauscher et al., 2004),
441 and chloroplast noncoding sequences (Hsing et al. 2001). The use of BEAST and *BEAST (Heled and Drummond,
442 2010) allowed us to estimate divergence times of alleles and species for the first time for some of these taxa. Dating
443 polyploid origins is complicated by numerous factors (Doyle and Egan, 2010). For one thing, if the polyploid has
444 arisen recurrently, then there is no single date that marks "the" origin. Given that polyploids are often invasive (e.g.,
445 Pandit et al., 2011), and the *Glycine tomentella* allopolyploids appear to be recently formed based on sharing
446 identical histone H3D and nrDNA ITS alleles with their putative progenitors (Doyle et al., 2002; Rauscher et al.,
447 2004), we have speculated that they could have originated as a response to ecological disturbance due to human
448 colonization of Australia, around 40,000 years ago (Hudjashov et al., 2007; Pugach et al., 2013). The relevant date
449 for testing this anthropogenic disturbance hypothesis would be the oldest origin of each polyploid. However, because
450 it is unlikely that a polyploid allele and any of a set of diploid progenitor alleles will coalesce at exactly the time of
451 polyploid origin, distances for any given polyploid event will be overestimates of the actual time of origin. Further
452 complicating matters, the error bars on our BEAST divergence estimates were large relative to the estimates
453 themselves. Nevertheless, because even the minimum estimates of allele divergences between diploids and
454 tetraploids are around 0.3 MY, it appears likely that these *G. tomentella* allopolyploids are hundreds of thousands
455 rather than tens of thousands of years old. *BEAST estimates should be averages of all origins of a polyploid taxon,
456 and these, too are several hundred thousand years for each allopolyploid. Thus, it appears likely that these polyploid
457 species were present in Australia before humans arrived there. The fact that these three species, and possibly other
458 allopolyploid members of the complex, may have evolved at roughly the same time is intriguing. In the ca. 5 MY
459 since the perennial members of *Glycine* diverged from the annual lineage (Egan and Doyle, 2010), there is no
460 evidence of polyploidy until these species were formed, apparently well within the last 1 MY. Perhaps the onset of
461 severe aridity in Australia around 3 MYA, heralding the change to the present extreme wet-dry glacial cycles (Crisp
462 et al., 2004) could have provided ecological opportunities for polyploids. It will be interesting to refine our estimates
463 through increased sampling of these three triads, and to obtain estimates for the other five allopolyploid species.

464 **ACKNOWLEDGEMENTS**

465 The authors thank Sue Sherman-Broyles for helpful comments throughout the project. We also are grateful to Steven
466 Cannon and a second, anonymous reviewer for detailed comments and suggestions.

467 REFERENCES

- 468 **Arnold B, Bomblies K, Wakeley J** (2012) Extending Coalescent Theory to Autotetraploids. *Genetics* **192**: 195–204
- 469 **Aronesty E** (2013) Comparison of sequencing utility programs. *Open Bioinform J.* **7**:1-8
- 470 **Blanc G, Wolfe K** (2004) Widespread paleopolyploidy in model plant species inferred from age distributions of
471 duplicate genes. *Plant Cell* **16**: 1667–1678
- 472 **Bombarely A, Edwards KD, Sanchez-Tamburrino J, Mueller LA** (2012) Deciphering the complex leaf
473 transcriptome of the allotetraploid species *Nicotiana tabacum*: a phylogenomic perspective. *BMC genomics* **13**:406
- 474 **Brown AHD, Doyle JL, Grace JP, Doyle JJ** (2002) Molecular phylogenetic relationships within and among
475 diploid races of *Glycine tomentella* (Leguminosae). *Australian Systematic Botany* **15**: 37–47
- 476 **Cannon SB, Ilut D, Farmer AD, Maki SL, May GD, Singer SR, Doyle JJ** (2010) Polyploidy did not predate the
477 evolution of nodulation in all legumes. *PLoS ONE* **5**: e11630
- 478 **Chester M, Gallagher JP, Symonds VV, Cruz da Silva AV, Mavrodiev EV, Leitch AR, Soltis PS, Soltis DE**
479 (2012) Extensive chromosomal variation in a recently formed natural allopolyploid species, *Tragopogon miscellus*
480 (Asteraceae). *Proc. Natl. Acad. Sci. U.S.A.* **109**: 1176–1181
- 481 **Coate JE, Doyle JJ** (2010) Quantifying whole transcriptome size, a prerequisite for understanding transcriptome
482 evolution across species: an example from a plant allopolyploid. *Genome Biol Evol* **2**: 534–546
- 483 **Coate JE, Doyle JJ** (2013) Genomics and transcriptomics of photosynthesis in polyploids. In *Polyploid and Hybrid*
484 *Genomics*, (Chen ZJ and Birchler JA, eds) Hoboken, NJ: Wiley-Blackwell, pp. 153–169
- 485 **Coate JE, Luciano AK, Seralathan V, Minchew KJ, Owens TG, Doyle JJ** (2012) Anatomical, biochemical, and
486 photosynthetic responses to recent allopolyploidy in *Glycine dolichocarpa* (Fabaceae). *Am J Bot* **99**: 55–67
- 487 **Coate JE, Powell AF, Owens TG, Doyle JJ** (2013) Transgressive physiological and transcriptomic responses to
488 light stress in allopolyploid *Glycine dolichocarpa* (Leguminosae). *Heredity* **110**: 160–170
- 489 **Coate JE, Bar H, Doyle JJ** (2014) Extensive translational regulation of gene expression in an allopolyploid
490 correlates with long term retention of duplicated genes. *The Plant Cell* **26**:136:150
- 491 **Crisp M, Cook L, Steane D** (2004) Radiation of the Australian flora: what can comparisons of molecular
492 phylogenies across multiple taxa tell us about the evolution of diversity in present-day communities? *Philos Trans R*
493 *Soc Lond, B, Biol Sci* **359**: 1551–1571
- 494 **Darlington CD** (1937) Recent advances in cytology. Second edition. Philadelphia. P. Blakiston's son and Co.
- 495 **Darriba D, Taboada GL, Doallo R, Posada D** (2012) jModelTest 2: more models, new heuristics and parallel
496 computing. *Nat Meth* **9**: 772
- 497 **Doyle JJ, Schuler MA, Godette WD, Zenger V, Beachy RN, Slightom JL** (1986) The glycosylated seed storage
498 proteins of *Glycine max* and *Phaseolus vulgaris*. Structural homologies of genes and proteins. *Journal of Biological*
499 *Chemistry* **261**(20):9228-38.
- 500 **Doyle JJ, Doyle JL, Brown AH** (1999) Origins, colonization, and lineage recombination in a widespread perennial
501 soybean polyploid complex. *Proc. Natl. Acad. Sci. U.S.A.* **96**: 10741–10745
- 502 **Doyle JJ, Doyle JL, Brown A, Palmer RG** (2002) Genomes, Multiple Origins, and Lineage Recombination in the

- 503 Glycine tomentella (Leguminosae) Polyploid Complex: Histone H3-D Gene Sequences. *Evolution*
- 504 **Doyle JJ, Doyle JL, Rauscher J, Brown A** (2004) Diploid and Polyploid Reticulate Evolution Throughout the
505 History of the Perennial Soybeans (Glycine Subgenus Glycine). *New Phytol* **161**: 121–132
- 506 **Doyle JJ, Egan AN** (2010) Dating the origins of polyploidy events. *New Phytol* **186**: 73–85
- 507 **Doyle JJ** (2012) Polyploidy in Legumes. In PS Soltis, DE Soltis, eds, *Polyploidy and Genome Evolution*. Springer
508 Berlin Heidelberg, Berlin, Heidelberg, pp 147–180
- 509 **Doyle MJ, Brown AHD** (1985) Numerical analysis of isozyme variation in *Glycine tomentella*. *Biochem Syst Ecol*
510 **13**: 413–419
- 511 **Doyle MJ, Grant JE, Brown AHD** (1986) Reproductive isolation between isozyme groups of *Glycine tomentella*
512 (Leguminosae) and spontaneous doubling in their hybrids. *Aust J Bot* **34**:523–535
- 513 **Drummond AJ, Suchard MA, Xie D, Rambaut A** (2012) Bayesian phylogenetics with BEAUti and the BEAST
514 1.7. *Mol Biol Evol* **29**: 1969–1973
- 515 **Du J, Tian Z, Sui Y, Zhao M, Song Q, Cannon SB, Cregan P, Ma J** (2012) Pericentromeric effects shape the
516 patterns of divergence, retention, and expression of duplicated genes in the paleopolyploid soybean. *Plant Cell* **24**:
517 21–32
- 518 **Dufresne F, Stift M, Vergilino R, Mable BK** (2014) Recent progress and challenges in population genetics of
519 polyploid organisms: an overview of current state-of-the-art molecular and statistical tools. *Mol Ecol* **23**: 40–69
- 520 **Edwards SV** (2009) Is a new and general theory of molecular systematics emerging? *Evolution* **63**: 1–19
- 521 **Egan AN, Doyle JJ** (2010) A comparison of global, gene-specific, and relaxed clock methods in a comparative
522 genomics framework: dating the polyploid history of soybean (*Glycine max*). *Syst Biol* **59**: 534–547
- 523 **Evanno G, Regnaut S, Goudet J** (2005) Detecting the number of clusters of individuals using the software
524 STRUCTURE: a simulation study. *Mol Ecol* **14**: 2611–2620
- 525 **Freeling M, Woodhouse MR, Subramaniam S, Turco G, Lisch D, Schnable JC** (2012) Fractionation mutagenesis
526 and similar consequences of mechanisms removing dispensable or less-expressed DNA in plants. *Curr Opin Plant*
527 *Biol* **15**: 131–139
- 528 **Gilad Y, Pritchard JK, Thornton K** (2009) Characterizing natural variation using next-generation sequencing
529 technologies. *Trends Genet* **25**: 463–471
- 530 **González-Orozco CE, Brown AHD, Knerr N, Miller JT, Doyle JJ** (2012) Hotspots of diversity of wild Australian
531 soybean relatives and their conservation in situ. *Conserv Genet* **13**: 1269–1281
- 532 **Grant JE, Brown AHD, Grace JP** (1984) Cytological and isozyme diversity in *Glycine tomentella* Hayata
533 (Leguminosae). *Aust J Bot* **32**:665–677
- 534 **Grover CE, Salmon A, Wendel JF** (2012) Targeted sequence capture as a powerful tool for evolutionary analysis.
535 *Am J Bot* **99**: 312–319
- 536 **Guindon S, Gascuel O** (2003) A simple, fast, and accurate algorithm to estimate large phylogenies by maximum
537 likelihood. *Syst Biol* **52**: 696–704
- 538 **Harbert RS, Brown AHD, Doyle JJ** (2014) Allopolyploidy, climate niche modeling, and evolutionary “success” in
539 *Glycine* (Leguminosae). *Am J Bot* **101**: 710–721
- 540 **Hegarty M, Coate J, Sherman-Broyles S, Abbott R, Hiscock S, Doyle J** (2013) Lessons from natural and artificial
541 polyploids in higher plants. *Cytogenet Genome Res* **140**: 204–225

- 542 **Heled J, Drummond AJ** (2010) Bayesian inference of species trees from multilocus data. *Mol Biol Evol* **27**: 570–
543 580
- 544 **Hollister JD, Arnold BJ, Svedin E, Xue KS, Dilkes BP, Bomblies K** (2012) Genetic adaptation associated with
545 genome-doubling in autotetraploid *Arabidopsis arenosa*. *PLoS Genet* **8**: e1003093
- 546 **Hsing Y-LC, Hsieh J-S, Peng C-L, Chou C-H, Chiang T-Y** (2001) Systematic Status of the *Glycine tomentella* and
547 *G. tabacina* Species Complexes (Fabaceae) Based on ITS Sequences of Nuclear Ribosomal DNA. *J Plant Res* **114**:
548 435–442
- 549 **Hudjashov G, Kivisild T, Underhill PA, Endicott P, Sanchez JJ, Lin AA, Shen P, Oefner P, Renfrew C, Villems**
550 **R, et al** (2007) Revealing the prehistoric settlement of Australia by Y chromosome and mtDNA analysis. *Proc. Natl.*
551 *Acad. Sci. U.S.A.* **104**: 8726–8730
- 552 **Huson DH, Bryant D** (2006) Application of phylogenetic networks in evolutionary studies. *Mol Biol Evol* **23**: 254–
553 267
- 554 **Hymowitz T, Singh RJ, Kollipara KP** (2010) The Genomes of the Glycine. *In Plant Breeding Reviews*. John Wiley
555 & Sons, Inc, Oxford, UK, pp 289–317
- 556 **Hut DC, Coate JE, Luciano AK, Owens TG, May GD, Farmer A, Doyle JJ** (2012) A comparative transcriptomic
557 study of an allotetraploid and its diploid progenitors illustrates the unique advantages and challenges of RNA-seq in
558 plant species. *Am J Bot* **99**: 383–396
- 559 **Innes RW, Ameline-Torregrosa C, Ashfield T, Cannon E, Cannon SB, Chacko B, Chen NWG, Couloux A,**
560 **Dalwani A, Denny R, et al** (2008) Differential accumulation of retroelements and diversification of NB-LRR
561 disease resistance genes in duplicated regions following polyploidy in the ancestor of soybean. *Plant Physiol* **148**:
562 1740–1759
- 563 **Jiao Y, Leebens-Mack J, Ayyampalayam S, Bowers JE, McKain MR, McNeal J, Rolf M, Ruzicka DR, Wafula**
564 **E, Wickett NJ, et al** (2012) A genome triplication associated with early diversification of the core eudicots. *Genome*
565 *Biol* **13**: R3
- 566 **Jiao Y, Wickett NJ, Ayyampalayam S, Chanderbali AS, Landherr L, Ralph PE, Tomsho LP, Hu Y, Liang H,**
567 **Soltis PS, et al** (2011) Ancestral polyploidy in seed plants and angiosperms. *Nature* **473**: 97–U113
- 568 **Joly S, Rauscher JT, Sherman-Broyles SL, Brown AHD, Doyle JJ** (2004) Evolutionary dynamics and preferential
569 expression of homeologous 18S-5.8S-26S nuclear ribosomal genes in natural and artificial glycine allopolyploids.
570 *Mol Biol Evol* **21**: 1409–1421
- 571 **Jones G, Sagitov S, Oxelman B** (2013) Statistical inference of allopolyploid species networks in the presence of
572 incomplete lineage sorting. *Syst Biol* **62**: 467–478
- 573 **Langmead B, Salzberg SL** (2012) Fast gapped-read alignment with Bowtie 2. *Nat Meth* **9**: 357–359
- 574 **Lawson DJ, Hellenthal G, Myers S, Falush D** (2012) Inference of population structure using dense haplotype data.
575 *PLoS Genet* **8**: e1002453
- 576 **Leitch IJ, Bennett MD** (2004) Genome downsizing in polyploid plants. *Biological Journal of the Linnean Society*
577 **82**:651–663
- 578 **Li H, Handsaker B, Wysoker A, Fennell T, Ruan J, Homer N, Marth G, Abecasis G, Durbin R, 1000 Genome**
579 **Project Data Processing Subgroup** (2009) The Sequence Alignment/Map format and SAMtools. *Bioinformatics* **25**:
580 2078–2079
- 581 **Lynch M, Conery JS** (2000) The evolutionary fate and consequences of duplicate genes. *Science* **290**: 1151–1155

- 582 **Maere S, De Bodt S, Raes J, Casneuf T, Van Montagu M, Kuiper M, Van de Peer Y** (2005) Modeling gene and
583 genome duplications in eukaryotes. *P Natl Acad Sci Usa* **102**: 5454–5459
- 584 **McClintock B** (1984) The significance of responses of the genome to challenge. *Science* **226**: 792–801
- 585 **Pandit MK, Pockock MJO, Kunin WE**, (2011) Ploidy influences rarity and invasiveness in plants. *J. Ecol.* **99**:1108-
586 1115.
- 587 **Pritchard J, Stephens M, Donnelly P** (2000) Inference of population structure using multilocus genotype data.
588 *Genetics* **155**: 945–959
- 589 **Pugach I, Delfin F, Gunnarsdottir E, Kayser M, Stoneking M** (2013) Genome-wide data substantiate Holocene
590 gene flow from India to Australia. *Proc. Natl. Acad. Sci. U.S.A.* **110**:1803-1808.
- 591 **Rambaut A** (2012) FigTree version 1.4.0. <http://tree.bio.ed.ac.uk/software/figtree/>
- 592 **Ramsey J, Schemske DW** (2002) Neopolyploidy in flowering plants. *Annu. Rev. Ecol. Syst.* **33**:589-639.
- 593 **Ratnaparkhe MB, Singh RJ, Doyle JJ** (2011) Glycine. *Wild Crop Relatives: Genomic and Breeding Resources,*
594 *Legume Crops and Forage*, C. Kole (ed.) Springer-Verlag Berlin Heidelberg, Berlin, Heidelberg, pp 83–116
- 595 **Rauscher JT, Doyle JJ, Brown AHD** (2004) Multiple origins and nrDNA internal transcribed spacer homeologue
596 evolution in the *Glycine tomentella* (Leguminosae) allopolyploid complex. *Genetics* **166**: 987–998
- 597 **Rauscher JT, Doyle JJ, Brown AHD** (2002) Internal transcribed spacer repeat-specific primers and the analysis of
598 hybridization in the *Glycine tomentella* (Leguminosae) polyploid complex. *Mol Ecol* **11**: 2691–2702
- 599 **Schlueter J, Dixon P, Granger C, Grant D, Clark L, Doyle JJ, Shoemaker R** (2004) Mining EST databases to
600 resolve evolutionary events in major crop species. *Genome* **47**: 868–876
- 601 **Schmutz J, Cannon SB, Schlueter J, Ma J, Mitros T, Nelson W, Hyten DL, Song Q, Thelen JJ, Cheng J, et al**
602 (2010) Genome sequence of the palaeopolyploid soybean. *Nature* **463**: 178–183
- 603 **Schnable JC, Freeling M** (2011) Genes identified by visible mutant phenotypes show increased bias toward one of
604 two subgenomes of maize. *PLoS ONE* **6**: e17855
- 605 **Shoemaker RC, Schlueter J, Doyle JJ** (2006) Paleopolyploidy and gene duplication in soybean and other legumes.
606 *Curr Opin Plant Biol* **9**: 104–109
- 607 **Singh RJ, Kim HH, Hymowitz T** (2001) Distribution of rDNA loci in the genus *Glycine* Willd. *Theor Appl Genet*
608 **103**: 212–218
- 609 **Singh RJ, Kollipara KP, Hymowitz T** (1998) The genomes of *Glycine canescens* FJ Herm., and *G. tomentella*
610 Hayata of Western Australia and their phylogenetic relationships in the genus *Glycine* Willd. *Genome* **41**:669-679
- 611 **Slotte T, Bataillon T, Hansen TT, St Onge K, Wright SI, Schierup MH** (2011) Genomic determinants of protein
612 evolution and polymorphism in *Arabidopsis*. *Genome Biol Evol* **3**: 1210–1219
- 613 **Slotte T, Hazzouri KM, Ågren JA, Koenig D, Maumus F, Guo Y-L, Steige K, Platts AE, Escobar JS, Newman**
614 **LK, et al** (2013) The *Capsella rubella* genome and the genomic consequences of rapid mating system evolution. *Nat*
615 *Genet* **45**: 831–835
- 616 **Soltis DE, Albert VA, Leebens-Mack J, Bell CD, Paterson AH, Zheng C, Sankoff D, dePamphilis CW, Wall**
617 **PK, Soltis PS** (2009) Polyploidy and angiosperm diversification. *Am J Bot* **96**: 336–348
- 618 **Soltis DE, Buggs RJA, Doyle JJ, Soltis PS** (2010). What we still don't know about polyploidy. *Taxon* **59**:1387-
619 1403.

- 620 **Symonds VV, Soltis PS, Soltis DE** (2010) Dynamics of polyploid formation in *Tragopogon* (Asteraceae): recurrent
621 formation, gene flow, and population structure. *Evolution* **64**: 1984–2003
- 622 **Trapnell C, Roberts A, Goff L, Pertea G, Kim D, Kelley DR, Pimentel H, Salzberg SL, Rinn JL, Pachter L**
623 (2012) Differential gene and transcript expression analysis of RNA-seq experiments with TopHat and Cufflinks. *Nat*
624 *Protoc* **7**: 562–578
- 625 **Trapnell C, Williams BA, Pertea G, Mortazavi A, Kwan G, van Baren MJ, Salzberg SL, Wold BJ, Pachter L**
626 (2010) Transcript assembly and quantification by RNA-Seq reveals unannotated transcripts and isoform switching
627 during cell differentiation. *Nat Biotechnol* **28**: 511–174
- 628 **Wang X, Tang H, Bowers JE, Feltus FA, Paterson AH** (2007) Extensive concerted evolution of rice paralogs and
629 the road to regaining independence. *Genetics* **177**: 1753–1763
- 630 **Wood TE, Takebayashi N, Barker MS, Mayrose I, Greenspoon PB, Rieseberg LH** (2009) The frequency of
631 polyploid speciation in vascular plants. *Proc. Natl. Acad. Sci. U.S.A.* **106**:13875–13879

Figure 1

Schema of the *Glycine* perennial polyploid complex.

Diploid progenitors are represented by circles and allotetraploid species by squares.

Chromosome numbers are shown for each species, and genome groups (Ratnaparkhe et al., 2011) are given for diploids. Species used in this study (*G. tomentella* D1, *G. tomentella* D3, *G. syndetika* D4, *G. canescens*, *G. clandestina*, *G. dolichocarpa* T2, *G. tomentella* T1 and *G. tomentella* T5) are shown in green.

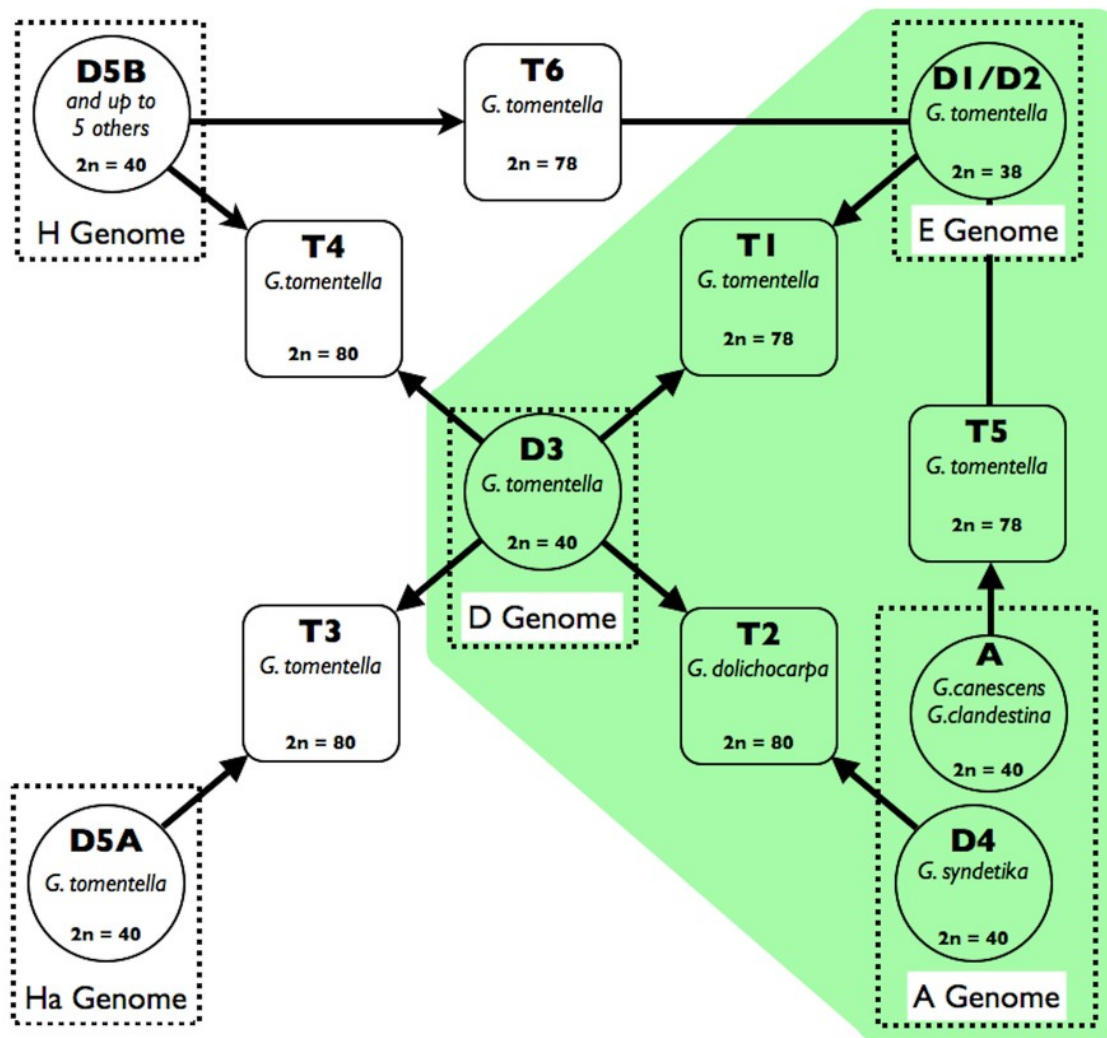


Figure 2

Electronic chromosome painting for *G. dolichocarpa* T2 accession 1134.

SNP positions on the 20 soybean chromosomes are represented by blue lines (D3 progenitor) or red lines (D4 progenitor).

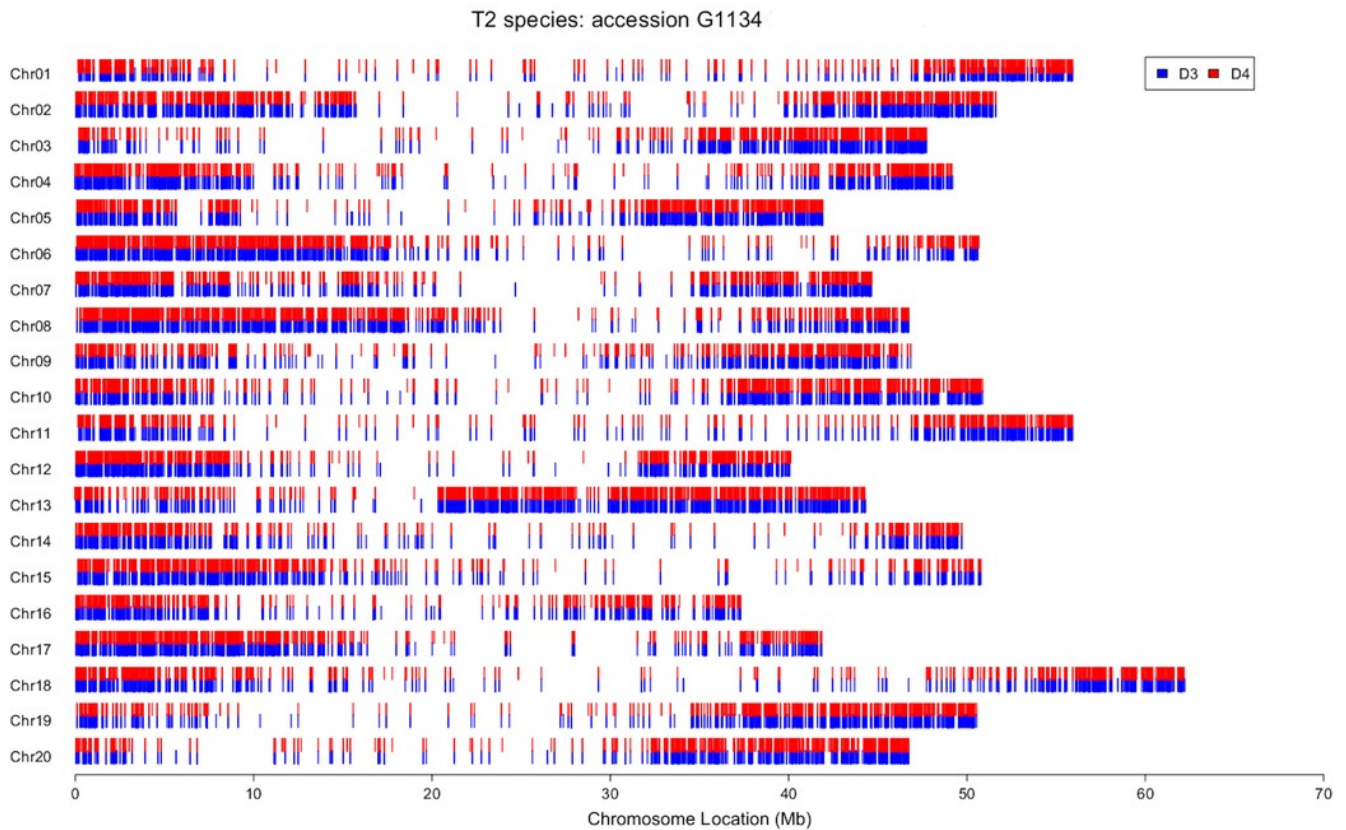


Figure 3

Structure analysis for *Glycine* perennial polyploid accessions

SNP analysis using Structure for a set of 20,000 random SNPs for *Glycine* polyploid complex accessions (A) without homoeologue separation and (B) with homoeologue separation for $K = 6$. The five progenitor diploid species are placed in different populations: red (*G. clandestina*), dark red (*G. canescens*), yellow (*G. tomentella D1*), blue (*G. syndetika D4*) and green (*G. tomentella D3*).

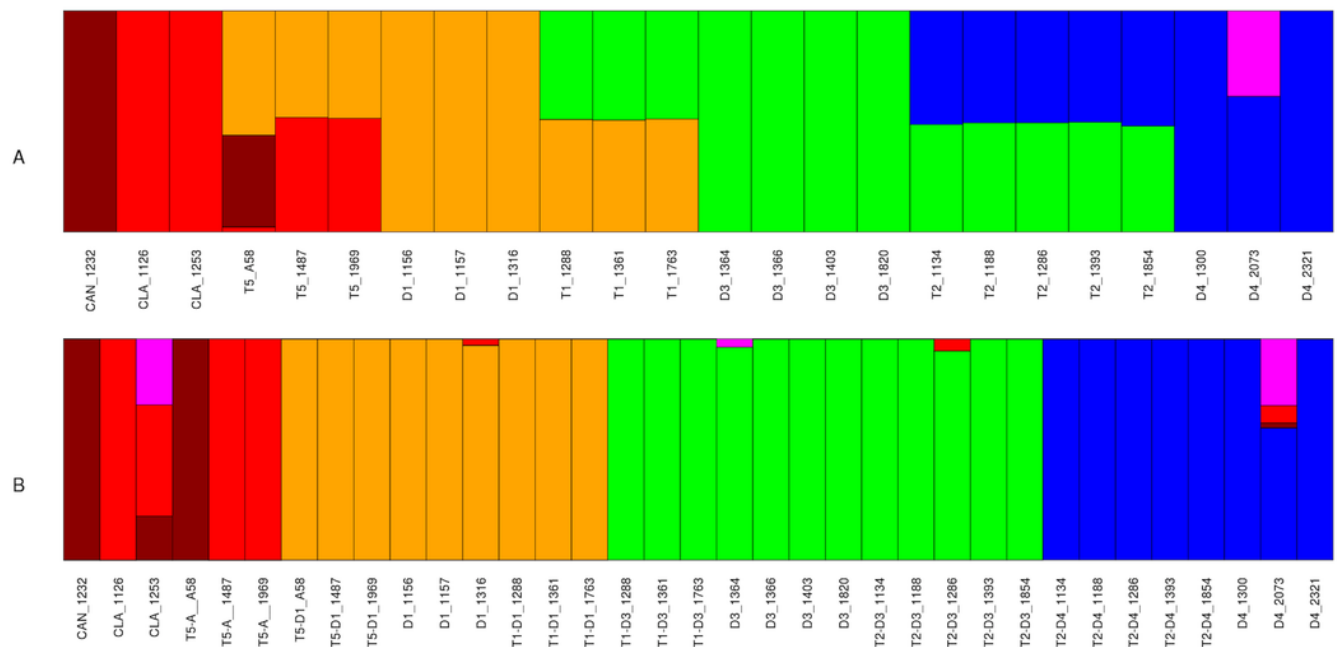


Figure 5

Phylogenetic relationship in the *Glycine* perennial polyploid complex

Relationships in the *Glycine* perennial polyploid complex after homoeologue separation, using a concatenated dataset. Branches are colored as in Fig. 4, based on the 5 different diploid species. In both the maximum likelihood (ML) phylogeny (A) and the NeighborNet network (B), the same major species groups are visible (D1, D3, D4 and *G. canescens*/*G. clandestina*).

Figure 6

Phylogenetic analysis for the Glyma02g11580 locus

Glyma02g11580 locus using ML with bootstrap values (A), NeighborNet (B), and BEAST with posterior probabilities and showing node ages (in black) (C). For figures A and C, branch length colors represent bootstrap or posterior probabilities values, with red shades being the lowest values and green shades being the highest values.

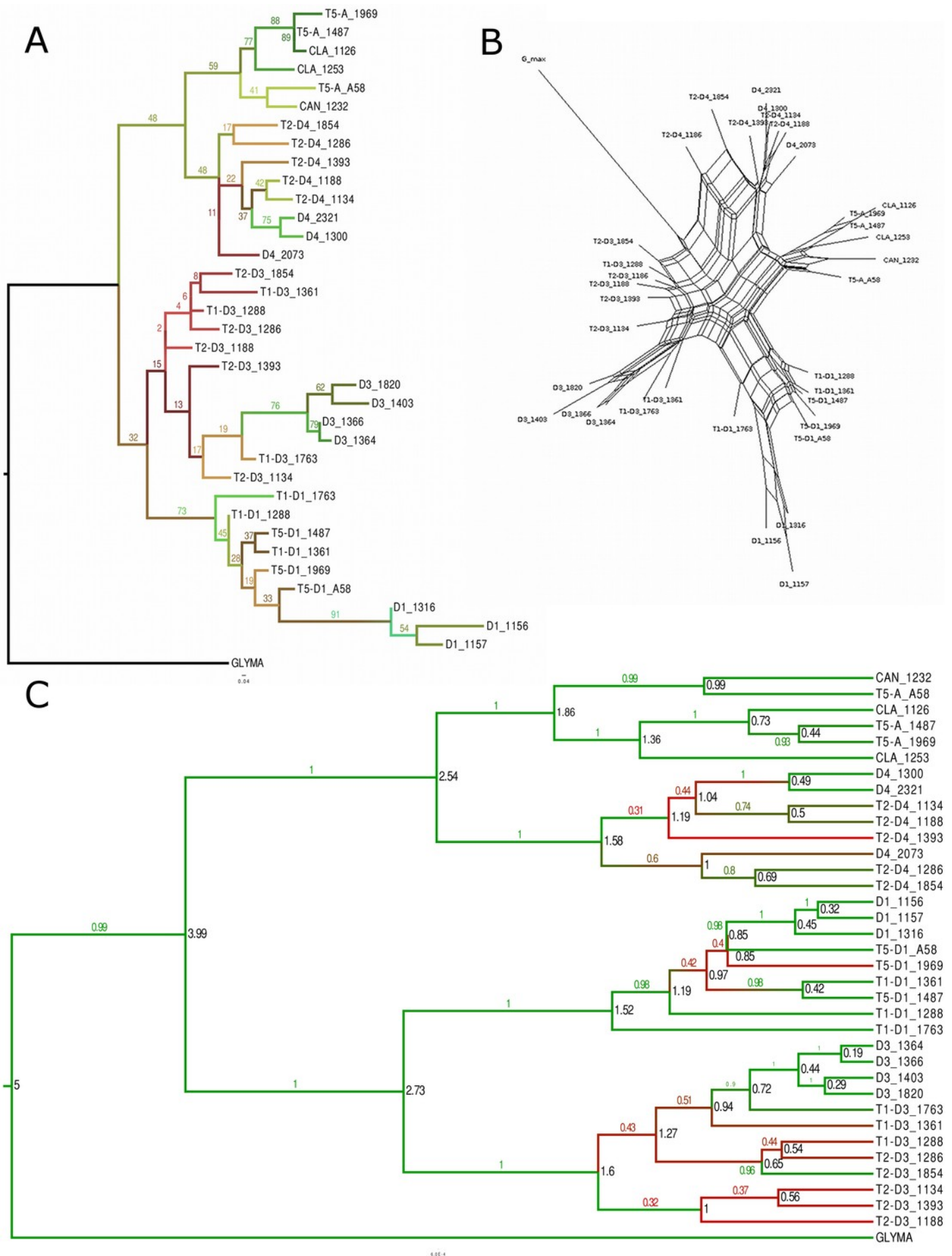


Figure 7

Phylogenetic tree with estimated divergence dates

*BEAST tree with the estimated node ages and error bars representing the highest posterior density (HPD) interval at the 95% level.

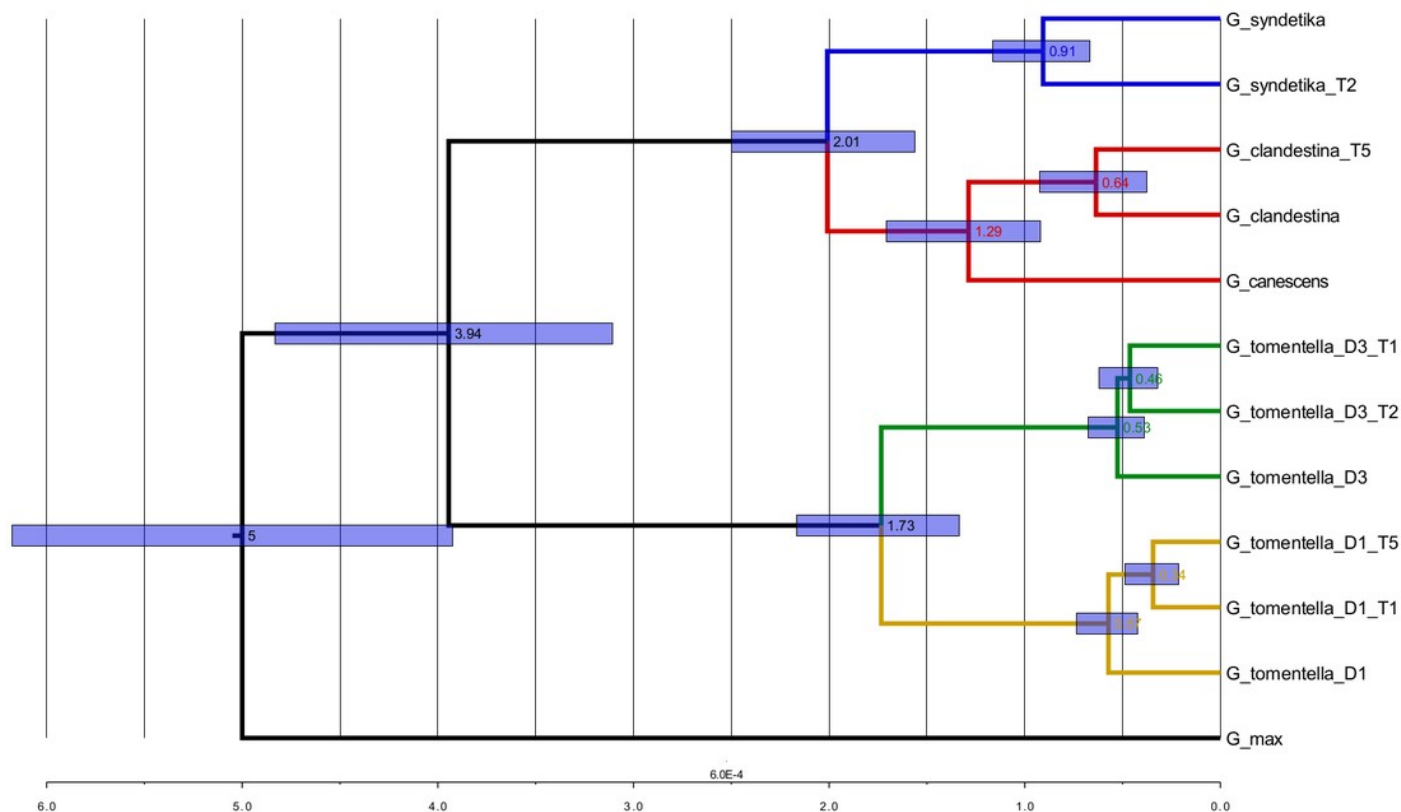


Table 1 (on next page)

Sequencing, reads processing and mapping summary.

Represented genes reflected the number of *Glycine max* reference genome genes where after the perennials reads mapping and expression measure have an expression > 0 (RPKM). Gray shading = allopolyploid species.

Species	Accession	Samples	Raw Reads	Processed Reads	Mapped Reads	Represented Genes
<i>Glycine canescens</i>	1232	2	21332880	20696801	14381555	23833
<i>Glycine clandestina</i>	1126	2	19086864	18613018	11815996	23340
	1253	3	33546015	32326942	19117095	23723
<i>Glycine dolichocarpa</i>	1134	13	202427873	187120918	60712525	23643
	1188	2	19034633	18279858	11960713	22952
	1286	2	11814995	11216980	7422888	25278
	1393	2	21820163	21029983	13643602	23345
	1854	3	54748079	42826840	16032643	22718
<i>Glycine syndetika</i>	1300	3	25527322	23634740	14092961	24238
	2073	2	12132989	11072073	7087710	24438
	2321	2	32796391	30024544	13637368	22571
<i>Glycine tomentella D1</i>	1156	3	38218179	36988846	21905536	23041
	1157	2	16522541	15906072	9715890	23920
	1316	2	25207045	24375482	15417078	22749
<i>Glycine tomentella D3</i>	1364	1	10401944	9604350	6896983	22802
	1366	2	20631583	18098232	10766169	23364
	1403	3	31631369	28953234	17218424	23352
	1820	3	71185274	63055644	18625439	22871
<i>Glycine tomentella T1</i>	1288	2	14608219	14148847	9298349	23348
	1361	2	17964870	17627119	11217736	23758
	1763	2	21870236	20933661	14101838	23349
<i>Glycine tomentella T5</i>	A58_1	2	22447334	21996303	13389955	23042
	1487	2	21267274	20469069	13907305	23437
	1969	3	21324229	20847883	11136293	23522

Table 2 (on next page)

Summary of SNPs using *G. max* as reference genome.

Gray shading = allopolyploid species. (* Between square brackets the coverage of the *G. max* transcriptome, including alternative splicings)(** Square brackets = percentage of heterozygous positions).

Species	Accession	% Gmax Coverage*	Raw SNPs	Processed SNPs**	Synonymous	Non-Synonymous
<i>Glycine canescens</i>	1232	7.2 [65.0]	589686	453,398 [7.7]	148321	123413
<i>Glycine clandestina</i>	1126	6.7 [61.4]	496746	375,943 [7.5]	115340	96562
	1253	7.5 [65.1]	617543	487,923 [8.3]	143952	124920
<i>Glycine dolichocarpa</i>	1134	11.6 [77.4]	1135676	965,643 [26.4]	242556	221326
	1188	7.4 [65.1]	550698	423,353 [28.9]	132471	113785
	1286	4.5 [45.5]	302661	224,653 [27.9]	67187	53595
	1393	6.7 [62.9]	470402	367,646 [28.8]	125339	104549
	1854	7.8 [65.3]	580531	471,020 [25.8]	140911	120274
<i>Glycine syndetika</i>	1300	7.5 [65.5]	605556	477,245 [7.8]	147362	125041
	2073	6.0 [57.6]	402798	282,215 [12.6]	91451	75333
	2321	8.0 [67.7]	670121	544,101 [6.3]	166409	143612
<i>Glycine tomentella D1</i>	1156	8.6 [69.7]	767614	621,043 [7.6]	190778	160781
	1157	6.2 [56.8]	455265	328,574 [7.1]	94377	77945
	1316	7.2 [62.3]	537439	412,518 [9.3]	120056	99666
<i>Glycine tomentella D3</i>	1364	5.0 [51.8]	335301	226,697 [7.8]	84917	65888
	1366	6.6 [59.7]	481258	360,327 [7.5]	111011	90015
	1403	6.4 [60.8]	476495	369,661 [6.6]	121526	99074
	1820	9.3 [69.6]	803774	641,145 [6.6]	188965	161826
<i>Glycine tomentella T1</i>	1288	6.9 [63.0]	498900	371,845 [19.6]	121418	102548
	1361	5.1 [54.2]	293339	200,738 [18.4]	75653	59378
	1763	7.1 [65.5]	533041	417,420 [19.4]	140203	116465
<i>Glycine tomentella T5</i>	A58_1	7.3 [64.6]	544331	430,552 [27.3]	135163	113781
	1487	7.0 [63.6]	516755	395,503 [26.8]	128199	105647
	1969	7.4 [65.9]	558920	444,468 [27.5]	146711	124933

Table 3(on next page)

Summary of the mapped reads and SNPs produced after the homoeologous reads separation.

It is based in the selective mapping with its progenitors (* Square brackets = percentage of heterozygous positions).

Species	Accession	Progenitor I Mapped to Progenitor I (%)	SNPs for I*	Progenitor II Mapped to Progenitor II (%)	SNPs for II*
<i>Glycine dolichocarpa</i>	1134	D3	11.4 399,884 [2.2]	D4	11.6 380,389 [2.1]
	1188	D3	20.8 227,610 [2.0]	D4	20.4 220,610 [2.1]
	1286	D3	20.3 124,984 [1.7]	D4	20.3 123,873 [1.8]
	1393	D3	19.6 197,132 [1.9]	D4	19.8 192,148 [1.9]
	1854	D3	17.9 245,354 [1.5]	D4	19.3 242,561 [1.7]
<i>Glycine tomentella T1</i>	1288	D1	14.9 143,232 [1.7]	D3	17.5 160,873 [1.9]
	1361	D1	15.0 155,360 [1.6]	D3	17.6 175,871 [2.0]
	1763	D1	14.8 158,777 [1.8]	D3	17.3 179,032 [2.0]
<i>Glycine tomentella T5</i>	A58_1	A	16.9 190,138 [2.1]	D1	20.5 222,134 [1.8]
	1487	A	17.1 174,051 [1.9]	D1	20.0 202,555 [1.7]
	1969	A	16.0 182,615 [2.4]	D1	18.6 214,799 [1.8]

Table 4 (on next page)

Summary of SNP count between species groups.

Polyploids are divided in two species according the progenitor origin. A Species includes *G. canescens*, *G. clandestina* and *G. tomentella* T5-A; D1 species includes *G. tomentella* D1, *G. tomentella* T1-D1 and *G. tomentella* T5-D1; D3 species includes *G. tomentella* D3, *G. tomentella* T1-D3 and *G. tomentella* T2-D3; D4 species includes *G. syndetika* and *G. tomentella* T2-D4. * The same species group contains the specific SNPs between accession of the same species.

Species Group	<i>Gmax</i> SNPs	A Group SNPs	D1 Group SNPs	D3 Group SNPs	D4 Group SNPs
A Species	9406	26,438 *	7096	6591	1465
D1 Species	11187	-	21,830 *	5933	7556
D3 Species	9299	-	-	25,157 *	7295
D4 Species	9314	-	-	-	23,324 *

Table 5(on next page)

Summary of the genes used in the BEAST and *BEAST analysis.

Tree likelihood values and the functional annotation are shown.

GeneID	TreeLikelihood Mean	TreeLikelihood ESS	Gene Functional Annotation
Glyma01g35620	-4676.067	1361.926	Phytoene dehydrogenase
Glyma02g11580	-3986.812	1034.414	RNA binding protein
Glyma03g29330	-7611.686	894.813	Magnesium chelatase
Glyma03g36630	-2666.725	696.197	Rho GTPase activating protein
Glyma04g39670	-4142.157	2556.251	ATP-binding transport protein-related
Glyma05g05750	-3028.809	541.483	Beta-amylase
Glyma05g09310	-2578.198	305.191	Pyruvate kinase
Glyma05g26230	-3741.498	5156.337	Metalloprotease M41 FtsH
Glyma05g37840	-2138.404	3766.767	Haloacid dehalogenase-like hydrolase
Glyma06g18640	-3418.91	6613.752	Elongation factor Tu
Glyma07g03370	-2091.845	742.796	Palmytoil-monogalactosyldiacylglycerol delta-7 desaturase
Glyma07g17180	-2218.934	2833.162	Fructose-1,6-bisphosphatase
Glyma10g42100	-2903.849	1774.192	3-ketoacyl-CoA synthase
Glyma11g13880	-4644.419	7487.252	Lipoxygenase
Glyma11g33720	-3592.689	2273.389	DELLA protein
Glyma12g04150	-2061.527	4777.335	Fructose-bisphosphate aldolase
Glyma12g12230	-2177.72	1790.185	O-methyltransferase
Glyma13g17820	-2439.715	342.999	Polyubiquitin
Glyma14g03500	-2063.541	819.216	Phytoene synthase
Glyma16g00410	-4041.294	4475.536	heat shock protein 70
Glyma16g01980	-4985.489	387.993	Myb-like protein
Glyma16g04940	-2152.355	4586.42	Glyceraldehyde 3-phosphate dehydrogenase
Glyma18g04080	-2285.776	9535.754	26S proteasome regulatory complex, ATPase RPT4
Glyma19g03390	-2344.831	3190.5	Unknown
Glyma19g32940	-2176.029	2579.558	Fatty acid desaturase
Glyma20g24930	-2803.585	6535.602	3-ketoacyl-CoA synthase
Glyma20g32930	-2867.321	2078.549	Cytochrome P450 77A3